IS THE POMERON NECESSARY AND IF SO WHY IS IT SO COMPLICATED?

Uri Maor

(Collaboration with E. Gotsman and E. Levin)

Raymond and Beverly Sackler Faculty of Exact Science

Tel Aviv University, Tel Aviv, 69978, Israel

EDS XIV BLOIS WORKSHOP

December 15-21, 2011. Qui Nhon, Vietnam

Introduction

Hard pQCD deals with high transverse momenta partons. These are short distance interactions calculated perturbatively.

Soft npQCD applies to low transverse momenta partons separated by large distances. The consequent phenomenological calculations are based foremost (but not only!) on the Regge pole model, in which the Pomeron ($I\!P$) is the leading term. It dominates soft scattering dynamics in the TeV range.

In the following I shall review the development of the Regge $I\!P$ to its present multi-layered structure. My main objective is to show that, regardless of its complexity, the updated $I\!P$ model provides a unique option for an overall description of soft scattering.

S-Channel Unitarity

The total and elastic (but NOT diffractive) cross sections in the ISR-Tevatron range are well reproduced by the DL model

$$\alpha_{I\!P}(t) = 1 + \Delta_{I\!P} + \alpha'_{I\!P} t, \quad \Delta_{I\!P} = 0.08, \quad \alpha'_{I\!P} = 0.25 GeV^{-2}.$$

Given a super critical $I\!P$ ($\Delta_{I\!P} > 0$), σ_{el} grows indefinitely faster than σ_{tot} and will, eventually, get larger! This paradox is eliminated by imposing an s-channel unitarity bound on $a_{el}(s,b)$.

Enforcing unitarity is model dependent. Start with a scattering matrix, where initial elastic re-scatterings secure s-unitarity

$$2Ima_{el}(s,b) = |\, a_{el}(s,b)|^2 + G^{in}(s,b).$$

This is no more than a statement that $\sigma_{tot}(s,b) = \sigma_{el}(s,b) + \sigma_{in}(s,b)$.

Its general solution is

$$a_{el}(s,b) = i\left(1 - e^{-\Omega(s,b)/2}\right) \quad \textbf{and} \quad G^{in}(s,b) = 1 - e^{-\Omega(s,b)}.$$

$\Omega(s,b)$ **is arbitrary, inducing a unitarity bound of** $|\, a_{el}(s,b)\,| \leq 2$.

In a Glauber type eikonal approximation the input opacity $\Omega(s,b)$ **is real. i.e.** $a_{el}(s,b)$ **is imaginary and it equals the imaginary part of the input Born term, a** $I\!P$ **exchange diagram in** $I\!P$ **models. The output bound is** $|\, a_{el}(s,b)\,| \leq 1$, **which is the black disc bound. The total, elastic and inelastic cross sections are given by**

$$\sigma_{tot} = 2\int d^2b\left(1 - e^{-\Omega(s,b)/2}\right),$$
$$\sigma_{el} = \int d^2b\left(1 - e^{-\Omega(s,b)/2}\right)^2,$$
$$\sigma_{inel} = \sigma_{tot} - \sigma_{el} = \int d^2b\left(1 - e^{-\Omega(s,b)}\right).$$

σ_{el} **is bounded by** $\sigma_{tot}/2$. **At the black disc bound** $\sigma_{el} = \sigma_{inel} = \sigma_{tot}/2$.

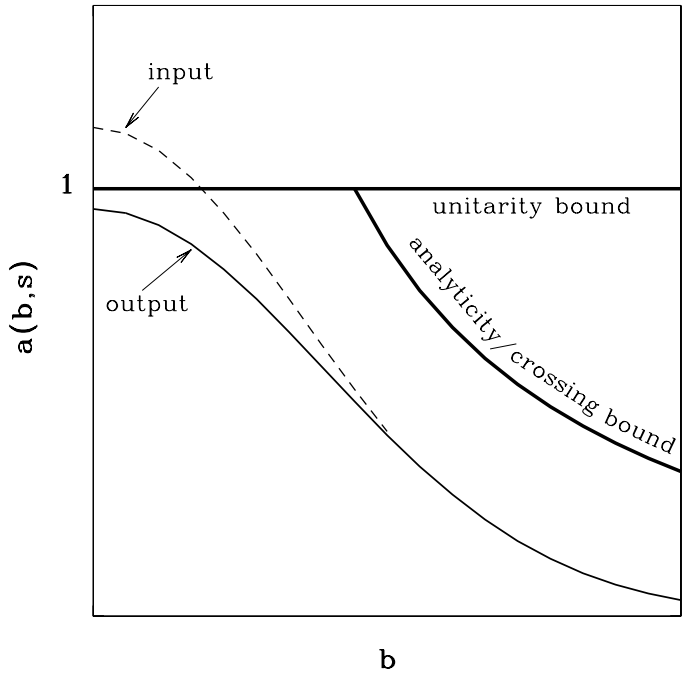

The figure shows the effect of eikonal screening securing that the screened elastic amplitude is s-unitarity bounded.

The figure illustrates, also, the bound on R^2_{el} implied by analyticity/crossing symmetry.

Saturating these bounds results in Froissart-Martin bound

$$\sigma_{tot} \leq Clog^2(s/s_0), \textbf{ in which } C = \pi/2m_\pi^2.$$

The coefficient C is far too large to make this bound useful.

One should remember that The Froissart-Martin $log^2 s$ behavior relates to the bound, NOT to the total cross section, as long as it is below the bound. Hence, a $log^2 s$ model behavior is compatible with, but NOT induced, by Froissart-Martin bound!

σ_{tot} is proportional to $d\sigma_{el}/dt$(t=0), i.e. a single point in t-space. σ_{tot} in b-space is obtained from a b^2 integration of the eikonal elastic b-amplitude. Consequently, b-unitarity saturation is a differential property. Indeed, small b saturation at LHC is very probable.

Good-Walker Mechanism

The physics presented in the previous chapter is deficient in two correlated fundamental elements which were ignored.

- **The roll played by the diffractive channels which are also $I\!P$ exchange processes.**
- **t-channel unitarity expressed through multi-$I\!P$ interactions.**

Consider a system of two orthonormal states, a hadron Ψ_h and a diffractive state Ψ_D. The GW mechanism stems from the observation that these states do not diagonalize the 2x2 interaction matrix T.

Assume that T is diagonalized by Ψ_1 and Ψ_2.

$$\textbf{we get,} \quad \Psi_h = \alpha\,\Psi_1 + \beta\,\Psi_2, \quad \Psi_D = -\beta\,\Psi_1 + \alpha\,\Psi_2, \quad \alpha^2 + \beta^2 = 1.$$

The 4 elastic (i,k) GW amplitudes are

$$A_{i,k}^{i',k'} = < \Psi_i \, \Psi_k | \mathbf{T} | \Psi_{i'} \, \Psi_{k'} >= A_{i,k} \, \delta_{i,i'} \, \delta_{k,k'}.$$

For initial $p(\bar{p}) - p$ we have $A_{1,2} = A_{2,1}$. The (i,k) s-channel unitarity equation is analogous to the single channel equation,

$$Im \, A_{i,k}(s,b) = |A_{i,k}(s,b)|^2 + G_{i,k}^{in}(s,b).$$

$G_{i,k}^{in}$ is the summed probability for all non GW inelastic processes, including non GW "high mass diffraction" induced by multi-$I\!P$ interactions. As in the single channel equation, we have

$$A_{i,k}(s,b) = i\left(1 - \exp\left(-\frac{\Omega_{i,k}(s,b)}{2}\right)\right), \quad G_{i,k}^{in}(s,b) = 1 - \exp\left(-\Omega_{i,k}(s,b)\right).$$

The opacities, $\Omega_{i,k}(s,b)$, are real, determined by the Born input. The resulting elastic, SD and DD amplitudes are:

$$a_{el}(s,b) = i\{\alpha^4 A_{1,1} + 2\alpha^2\beta^2 A_{1,2} + \beta^4 A_{2,2}\},$$
$$a_{sd}(s,b) = i\alpha\beta\{-\alpha^2 A_{1,1} + (\alpha^2 - \beta^2)A_{1,2} + \beta^2 A_{2,2}\},$$
$$a_{dd} = i\alpha^2\beta^2\{A_{1,1} - 2A_{1,2} + A_{2,2}\}.$$

Updated eikonal models are two channeled in which:

$\Omega_{i,k}(s,b) = \nu_{i,k}(s)\,\Gamma_{i,k}(s,b)$**.** **In Regge type models,** $\nu_{i,k}(s) = g_i g_k (\frac{s}{s_0})^{\Delta_{I\!P}}$**.**

$\Gamma_{i,k}(s,b)$ **is parametrized so as to reproduce the elastic and diffractive channels** $\frac{d\sigma}{dt}$ **in the forward cone.**

The eikonal re-scatterings of the incoming projectiles are summed over the GW eigen states.

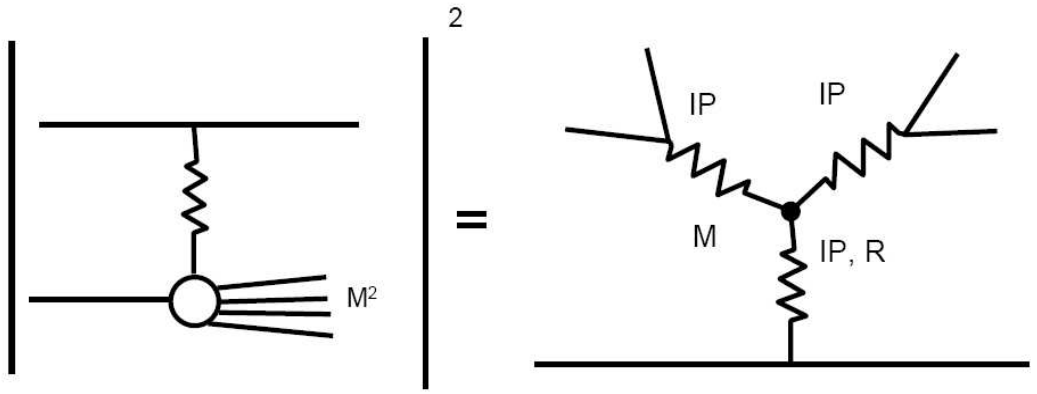

Multi-Pomeron Interactions

Mueller(1971) applied 3 body unitarity to equate the cross section

$a + b \to M + b$ **to the triple Regge diagram** $a + b + \bar{b} \to a + b + \bar{b}$.

The core of this representation is a triple vertex with a leading $3\mathbb{P}$ **term. The equation is valid for "high mass diffraction"**

$\frac{m_p}{M^2} << 1$ **and** $\frac{M^2}{s} << 1$.

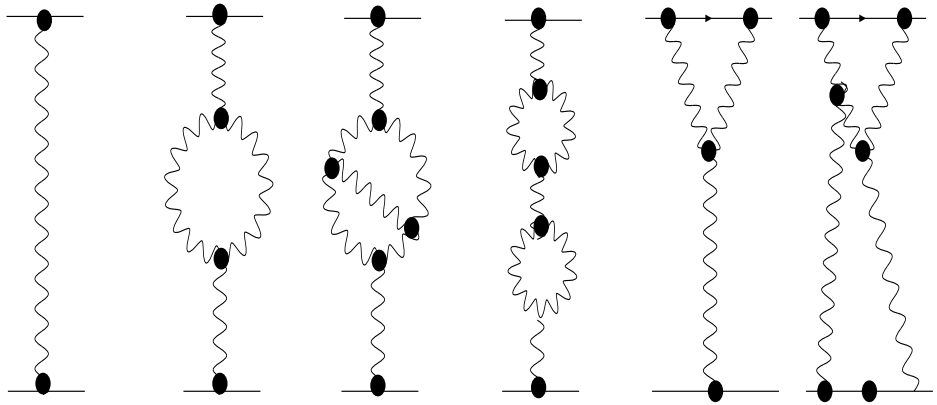

Muller's $3\mathbb{P}$ approximation for "high mass" single diffraction is the lowest order of a very large family of multi-$\mathbb{P}$ interactions which are not included in the GW mechanism. This dynamical feature is compatible with t-channel unitarity. The figure shows the low order $\mathbb{P}$ Green's function.

a) Enhanced diagrams which renormalize the $\mathbb{P}$ propagator.

b) Semi-enhanced diagrams which renormalize the p-$\mathbb{P}$-p vertexes.

In as much as the concept of "low" and "high mass" diffraction is 40 years old, we are still confronted with ambiguities in both its theoretical calculations and experimental definitions.

- **The complexity of the multi-$I\!P$ diagrams results in model dependent summing.**
- **Commonly, "high mass diffraction" lower bound is Y = 3, corresponding to $M^2 = 20GeV^2$. Its upper bound is $M^2 = 0.05s$.**
- **Kaidalov(1986) "low mass diffraction" upper bound is Y = 3, with no overlap between "low" and "high mass diffraction." This is assumed also by KMR and Ostapchenko.**

- The approach of GLM is radically different. Both GW and non GW diffraction have the same upper bound. Consequently, GLM diffraction has a large GW component, while Kaidalov, KMR and Ostapchenko are richer in non GW diffraction.
- In the ISR- Tevatron range the difference between the two definitions is relatively small. At LHC energies the difference becomes more significant.
- Regardless of the above, the updated $I\!P$ model is the only option in the market that offers a procedure which is compatible with t-channel unitarity.

Exceedingly High Energy Behavior

The definitions of GW and non GW diffraction have profound implication on the exceedingly high energy approach toward the black disc bound.

Single channel models neglect the GW mixing of the elastic and "low mass" diffractive wave functions. Consequently, their diffraction is "high mass" by default.

In a single channel non GW model, $\sigma_{el} \leq \frac{1}{2}\sigma_{tot}$. Equality is reached at the saturated black disc bound, where $\sigma_{el} = \sigma_{inel} = \frac{1}{2}\sigma_{tot}$.

In GW multi-channel models we distinguish between GW and non GW diffraction. Accordingly, we obtain the Pumplin bound $(\sigma_{el} + \sigma_{diff}^{GW}) \leq \frac{1}{2}\sigma_{tot}$. Equality is attained at the black disc saturation.

The implication is that in a multi-channel GW model,

$$\sigma_{el} \leq \tfrac{1}{2}\sigma_{tot} - \sigma_{diff}^{GW}, \qquad \sigma_{inel} \leq \tfrac{1}{2}\sigma_{tot} + \sigma_{diff}^{GW}.$$

In a recent publication, Block and Halzen analyzed an AUGER event for which they obtain: $\frac{\sigma_{inel}}{\sigma_{tot}} = 0.509 \pm 0.011$ **at** $W = 57 \pm 6 TeV$. **They conclude that the elastic and inelastic amplitudes are equal and saturated at this energy.**

As I have just shown, such a conclusion is valid only in single channel models, where the bounds on σ_{el} **and** σ_{inel} **are equal. This is not the case in multi-channel GW models, where the two bounds are different. Be reminded that in updated** $I\!P$ **models, such as GLM and KMR,** σ_{diff}^{GW} **is estimated at 50-60 TeV to be 15-20% of the inelastic cross section.**

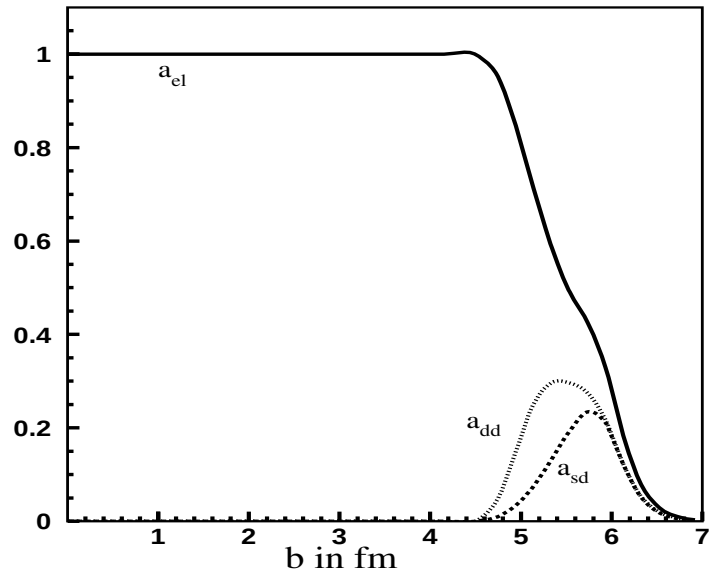

The basic GW amplitudes are $A^S_{1,1}$, $A^S_{1,2}$ and $A^S_{2,2}$. These are the building blocks with which we construct a_{el}, a_{sd} and a_{dd}. The $A^S_{i,k}$ amplitudes are bounded by the unitarity black disc bound of unity. $a_{el}(s,b)$ reaches this bound at a given (s,b) when, and only when, $A^S_{1,1}(s,b) = A^S_{1,2}(s,b) = A^S_{2,2}(s,b) = 1$, independent of the value of β. Consequently, when $a_{el}(s,b) = 1$, $a_{sd}(s,b) = a_{dd}(s,b) = 0$.

Lets re-check the diffractive channels at exceedingly high energies.

The elastic amplitude which is essentially black, has a high b tail where $a_{el}(s,b) < 1$**.**

In this domain diffraction can survive.

The Figure shows the elastic, SD and DD amplitudes at the Planck scale.

Updated Pomeron Model

The simple DL $I\!P$ model has evolved into a multi-layered model.

- **A bare non screened Pomeron exchange amplitude.**
- **The incoming projectiles eikonal re-scatterings initiate the screenings of the GW elastic and "low mass" diffraction amplitudes.**
- **t-channel unitarity is coupled to multi-$I\!P$ interactions, leading to "high mass" diffraction and renormalization of the Pomeron which screens the GW and non GW amplitudes.**
- **Survival probability has GW and non GW components which initiate further suppression of non GW diffraction.**

- **Current $I\!P$ models obtain a large $\Delta_{I\!P}$ and a diminishing $\alpha'_{I\!P}$. In the clasic Regge model $\Delta_{I\!P}$ controls the energy dependence of the scattering amplitudes, whereas $\alpha'_{I\!P}$ controls the shrinkage of the forward cones. These features are initiated in the updated $I\!P$ model through s and t screenings.**

The Partonic Pomeron

The microscopic sub structure of the Pomeron is provided in Gribov partonic interpretation of Regge theory, in which the slope of the Pomeron trajectory is related to the mean transverse momentum of the partonic dipoles constructing the Pomeron, and consequently, the running QCD coupling constant.

$$\alpha'_{I\!P} \propto 1/ < p_t >^2, \quad \alpha_S \propto \pi / ln\left(< p_t^2 > / \Lambda^2_{QCD} \right) << 1.$$

These observations intuitively suggest some connections between the soft and hard Pomerons. which is utilized in $I\!P$ models.

- **GLM utilize the pQCD MPSI procedure, where $nI\!P \to mI\!P$ reduces to a sequence of $G_{3I\!P}$ vertexes (Fan diagrams). i.e. $2I\!P \to I\!P$ and $I\!P \to 2I\!P$.**

- KMR couplings are $g_m^n = \frac{1}{2}\, g_N\ nm\, \lambda^{n+m-2} = \frac{1}{2}\, nm\, G_{3I\!P}\, \lambda^{n+m-3}$.

  λ **is a free parameter,** $n+m > 2$, $G_{3I\!P} = \lambda g_N$.

  Kaidalov and Ostapchenko have a different normalization.

Following I shall discuss 4 $I\!P$ **models. The models are conceptually similar, but differ in their** $I\!P$ **features.**

- GLM (Tel AVIV): **has a single soft** $I\!P$, $\Delta_{I\!P} = 0.20 - 0.30$, $\alpha'_{I\!P} \simeq 0$.
- KMR (Durham): $\Delta_{I\!P} = 0.3$, $\alpha'_{I\!P} \propto 1/p_t^2$.
- Ostapchenko (Bergen): **has 2 Pomerons,**

  soft: $\Delta_{I\!P} = 0.17$, $\alpha'_{I\!P} = 0.11$, **hard:** $\Delta_{I\!P} = 0.31$, $\alpha'_{I\!P} = 0.085$.
- Kaidalov-Poghosyan (Moscow): **is a single channel** $I\!P$ **model with**

  secondary Regge poles, $\Delta_{I\!P} = 0.12$, $\alpha'_{I\!P} = 0.22$.

How Many Pomerons

The Pomeron is void of electrical and color charges, is described as a 2 gluon color singlet. This is a Born term description.

In high order the 2 gluons are replaced by gluonic ladders.

The experimental study of e-p DIS provides a "laboratory" in which we can investigate the Pomeron properties as a function of its kinematic variables. Indeed, HERA e-p DIS data is a rich source of information on $I\!P$ features.

pQCD study of e-p DIS, in the limit of high Q^2 and exceedingly small x, led to the introduction of the hard BFKL Pomeron, corresponding to a hard gluon ladder.

- **The soft $I\!P$ is a simple moving pole in the J-plane, while, the BFKL $I\!P$ is a branch cut.**
- **The BFKL $I\!P$ is commonly parametrized as a simple J-pole with $\alpha'_{I\!P} = 0$, which is a signature of the hard $I\!P$.**
- **Recall that in pQCD the BFKL Pomeron slope $\alpha'_{I\!P} \propto 1/Q_s^2 \to 0$ as $s \to \infty$. Q_s^2 is the saturation scale.**

The figure presents $\sigma(\gamma^* + p \to p + X) \propto s^{\lambda}$. $\lambda = \Delta_{I\!P}$.

It shows the transition from the soft (non perturbative) Pomeron to the hard (perturbative) Pomeron.

As seen, at very small Q^2, $\Delta_{I\!P} \simeq 0.1$, compatible with the hadronic soft data. At higher Q^2, up to $\simeq 100\,GeV^2$, $\Delta_{I\!P}$ grows smoothly toward $\Delta_{I\!P} \simeq 0.30 - 0.35$.

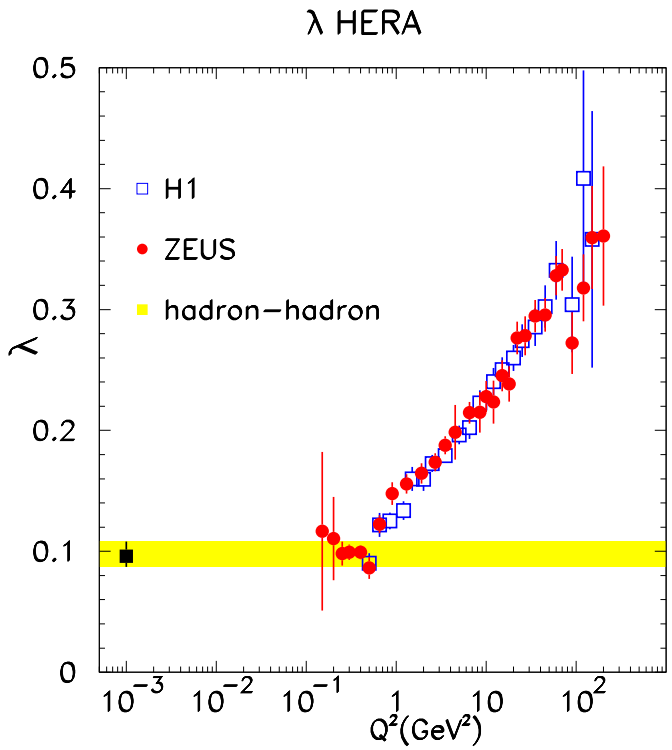

The basic input parameters of the soft and hard $I\!P$ are similar.

- **Even though the soft $I\!P$ parameters are model dependent, we can identify a common pattern,**

$\alpha'_{I\!P}$ **is small and** $\Delta_{I\!P}$ **is large.**

Given the strong screening induced by these parameters, the effective values of these parameters in the ISR-Tevatron range are compatible with DL.

- The parameters of the hard BFKL Pomeron are: $\alpha'_{I\!P} = 0$, reflecting the high p_t of the hard $I\!P$ partons. $\Delta_{I\!P}$ is large, determined by the pQCD calculations.
  In NLO: $\Delta_{I\!P}^{BFKL} \simeq 0.20 - 0.35$, depending on the renormalization scheme used.

- the triple $I\!P$ vertex plays an important roll in multi Pomeron interactions. Its value is determined by the data analysis.

- Even though, the 3 multi channel models differ in their $I\!P$ model details, their output is consistent with the HERA figure.

LHC Cross Section Data

1) Inclusive Pseudorapidity Distributions:

NSD data on charged multiplicity density distribution

$$dN_{ch}/d\eta \; = \; 1/\sigma_{NSD} d\sigma/d\eta$$

has been published by ALICE, CMS and ATLAS at central pseudorapidity $-2.5 \leq \eta \leq 2.5$**.**

This data provides an additional perspective on the $I\!P$ **model.**

In the framework of Gribov's $I\!P$ **calculus, single inclusive cross sections can be calculated using Mueller diagrams. To this end we have utilized the fitted parameters of the GLM** $I\!P$ **model.**

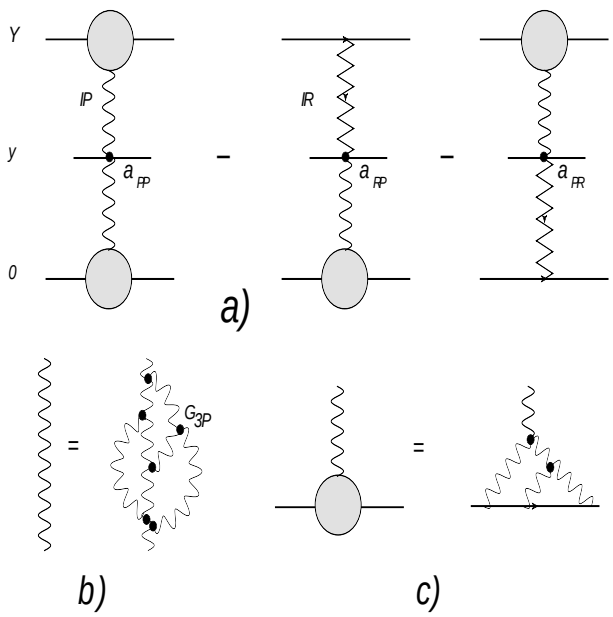

We add 3 phenomenological parameters:

$a_{I\!P I\!P}$ **and** $a_{I\!P R} = a_{R I\!P}$**, which account for hadron emission from the exchanged** $I\!P$ **or Reggeon. Q is the average transverse momentum of the produced mini-jets.**

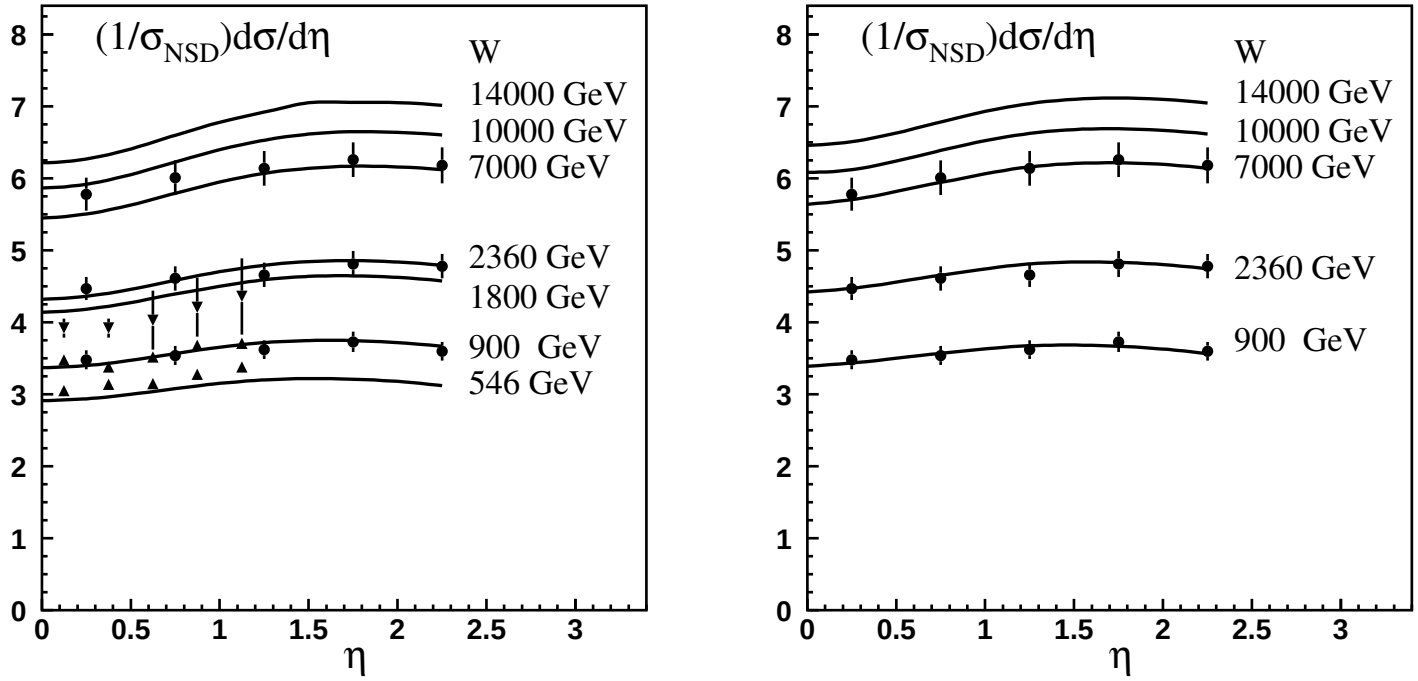

The data base for this fit is obtained from experiments spread over many years with different approaches to their analysis. We have fitted first the 546, 900, 1800, 2369, 7000 GeV data.

The second fit was confined to the very recent CMS data at 900, 2360, 7000 GeV.

The two sets of fitted parameters are close but not identical.

Our results are significant, in as much, as we offer a consistent reproduction of the SppS-Tevatron-LHC inclusive data.

ATLAS	ALICE	CMS	TOTEM
$69.4 \pm 2.4 \pm 6.9$	$72.7 \pm 1.1 \pm 5.1$	$71.8 \pm 1.1 \pm 2.0 \pm 7.9$	$73.5 \pm 0.6 + 1.8 - 1.3$

TABLE I: LHC σ_{inel} at 7 TeV

Achilli et al.	Block-Halzen	GLM	Kaidalov-Poghosyan	KMR
60-75	69.0	68.3	70.0	62.6-67.1

TABLE II: σ_{inel} model predictions at 7 TeV

2) Inelastic Cross Sections:

Cross sections contributing to σ_{tot} are $\sigma_{tot} = \sigma_{el} + \sigma_{sd} + \sigma_{dd} + \sigma_{nd}$.

The first measurements of the inelastic cross section derive from the minimum bias data samples. σ_{inel} can be directly determined by $\sigma_{inel} = \sigma_{tot} - \sigma_{el}$, provided both σ_{tot} and σ_{el} are measured.

The 2 tables above compare the 7 TeV σ_{inel} data and model predictions.

	TOTEM	ATLAS	CMS
σ_{tot}mb	98.3±0.2±2.7+0.8-0.2	96.0±3.3±9.5	94.0±2.8±5.5
σ_{el} mb	24.8±0.2±2.8	26.6	22.2

TABLE III: LHC σ_{tot} and σ_{el}.

	Achilli et al.	Block-Halzen	Halzen-Igi et al.	GLM	KP	KMR
σ_{tot}mb	91.6	95.4	96.1	91.3	96.4	89.0
σ_{el} mb		26.4		23.0	24.8	21.9

TABLE IV: σ_{tot} and σ_{el} theoretical predictions.

3) Total And Elastic Cross Sections

The tables compare σ_{tot} and σ_{el} at 7 TeV with theoretical model predictions.

Discussion

In this talk I have related to two theoretical options to describe soft scattering at very high energies.

- updated $I\!P$ models: GLM, KMR and Ostapchenko. These are 2 channel GW models.
- Kaidalov-Poghosyan follows a similar concept in a non GW single channel model.
- Block-Halzen-Igi-Pancheri et al. have presented similar mini-jets non Pomeronic single channel models which refrain from dealing with diffraction.

Updated $I\!P$ models cross section predictions at 7 TeV are moderately lower than the LHC data, which is well reproduced by the sibgle channel models of Block-Halzen-Igi et al. and Kaidalov-Poghosyan.

Note that, all σ_{tot} values obtained by the LHC groups are larger than the DL prediction of 90.7mb.

The problem with the $I\!P$ models can be traced to the fact that their complexity requires a large number of free parameters, in no proportion to their small data base.

GLM confronted this problem by enlarging their data base with ISR data. As such, the low energy ISR data "controls" the fit.

The same problem was confronted differently by KMR and Ostapchenko, who tuned, rather than fitted their data base.

In my opinion, all 3 groups should be more innovative in their statistical methods and better tune their output! Clearly the strength of these models is that they confront the issue of s and t unitarity.

The issue with the non GW single channel models is fundamental. As it stands, a non GW diffraction is "high mass", even though, the diffractive data obviously has also a "low mass" component. Recall that, Block-Halzen-Igi-Pancheri ignore the issue of diffraction all together.